ISSN(Online): 2320-9801
ISSN (Print): 2320-9798

International Journal of Innovative Research in Computer and Communication Engineering

(An ISO 3297: 2007 Certified Organization)

Website: www.ijircce.com

Vol. 5, Issue 4, April 2017

Co-Simulation of a BLDC motor with a front end converter using an FPGA based controller in MATLAB/SIMULINK and Xilinx System Generator

Veena P, Shubha Rao K

PG Scholar, Department of Electrical and Electronics, B N M Institute of Technology, Bengaluru, India

Associate Professor, Department of Electrical and Electronics, B N M Institute of Technology, Bengaluru, India

ABSTRACT: This paper focus on a novel operation of a brushless dc (BLDC) motor fed by a proportional integral (PI) controlled buck-boost converter supplemented with a battery to provide the required power to drive the BLDC motor. The operational characteristics of the proposed BLDC motor drive system for constant as well as step changes in dc link voltage of a front end converter controlled by a Xilinx System Generator (XSG) based PI controller for two quadrant operations are derived. Thus field programmable gate array (FPGA) based PI controller manages the energy flow through the battery and the front end converter. Moreover, speed to voltage conversion logic, made to control the BLDC motor through the PI controller, improves the performance and gives optimum control under the unstable driving situation or varying load condition when the complete system becomes a subject of application to electric vehicles (EVs) and hybrid electric vehicles (HEVs). The dual closed loop control implemented for end to end speed control of the proposed drive system facilitates the system with high accuracy integrated with excellent dynamic and steady state performance. In this paper, the proposed controller was designed for a 5 kW/480 V BLDC motor drive system. The feasibility of the proposed dual loop control topology for the BLDC motor drive system is validated and verified with extensive dynamic simulation in MATLAB/SIMULINK and XSG environment.

KEYWORDS: BLDC motor drive, EVs, FPGA, front end converter, HEVs, PI controller, Xilinx system generator (XSG)

I. INTRODUCTION

Over the last two decades, issues like sustainable development and environmental pollution due to vehicular emissions are accelerating modern science and technology and have given thrust to the research on electric vehicles (EVs) and hybrid electric vehicles (HEVs). Brushless dc (BLDC) motor drives have been found more suitable for EVs, HEVs, and other low power applications [1{3]. The BLDC motor has many advantages over the conventional induction and dc motors, such as better speed and torque characteristics, high efficiency and reliability, low electromagnetic interference (EMI), high power to weight and torque to current ratio, and long operation life [4,5]. Compared to induction machines the BLDC motor has lower inertia, allowing for faster dynamic response to reference commands. Moreover, advancements in power electronic devices and DSP/FPGA based processors have added more features to these motor drives to make them more prevalent in industrial installations [6{8]. Hysteresis current control and pulse width modulation (PWM) control coupled with continuous control theory produced the most widely used BLDC motor control techniques. The control of a BLDC motor in medium as well as high speed applications is much easier compared to induction motors.

Hysteresis current control is essential in achieving adequate control of instantaneous torque and hence yielding faster speed response. Digital PWM control techniques implemented for speed control of BLDC motors have maximum

ISSN(Online): 2320-9801
ISSN (Print): 2320-9798

International Journal of Innovative Research in Computer and Communication Engineering

(An ISO 3297: 2007 Certified Organization)

Website: www.ijircce.com

Vol. 5, Issue 4, April 2017

speed error below 5%. Therefore, they are not suitable for applications that require high precision. Conduction angle control and current mode control of BLDC motors also have significant errors in speed control, though less than those of digital PWM control. Conventional BLDC motors with a six switch inverter, excited through bipolar based soft switching currents, are suitable for low/medium power and medium speed applications as well. In order to use these motors effectively at their optimal efficiency and in the safe operating zone they must be driven at their nominal power requirement. Power electronic converters provide the featured solution to meet the demand for regulated electrical power for efficient and dynamic operation of BLDC motor drives. Most of the controllers designed for speed control of BLDC motors consider the unidirectional power converter as it facilitates the easy control and reduced cost of the drives. Moreover, the use of the battery to feed to the front end converter of the BLDC motor drive not only removes the lack of specific power, but also enables excellent performance of the drive system in both acceleration and regenerative braking in EV applications. The converter also adjusts the dc input voltage to the front end converter of the BLDC motor verses the motor speed in order to reduce the ripple of the motor current waveform. This fact is of particular importance in the case of slotless axial-flux PMDC motor drives, which have been proposed recently for medium-speed and high torque motor drive applications such as the direct driving of EV wheels. Conventional proportional integral (PI) control technology does not meet the requirement of a very fast dynamic response of EVs under rapid changes in operating modes of the drive system. The evolution of a high speed and high density FPGA based processor is now providing the best alternative to the ASIC and microprocessor based implementation of complex control algorithms. The improved and appreciable dynamic and steady state performance of BLDC motors supplemented with FPGA based controllers will make them suitable for position control in machine tools, robotics and high precision servos, aerospace, healthcare/biomedical equipment, speed control, and torque control in various industrial drives and process control applications.

II. STATE SPACE MODEL OF BUCK BOOST CONVERTER

The fundamental representation of state space modeling is

$$x' = Ax + Bu \quad (1)$$

$$y = Cx + Du \quad (2)$$

The buck-boost converter circuit and it's ON state and OFF state are shown in figure1

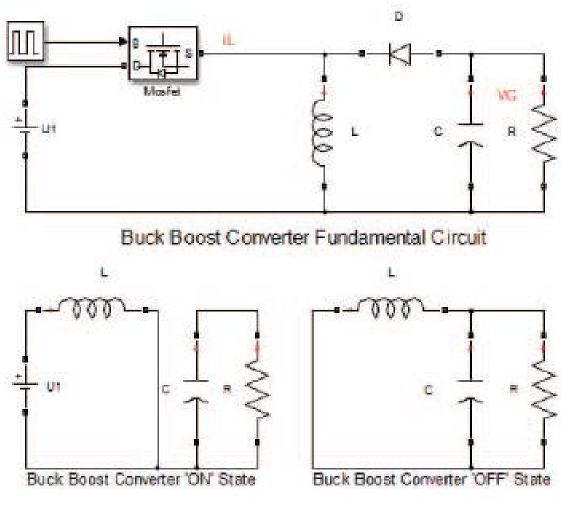

Figure1: Buck-Boost Converter, On State and Off State Equivalent Circuit

ISSN(Online): 2320-9801
ISSN (Print): 2320-9798

International Journal of Innovative Research in Computer and Communication Engineering

(An ISO 3297: 2007 Certified Organization)

Website: www.ijircce.com

Vol. 5, Issue 4, April 2017

When the switch is ON the inductor gets charged through the input voltage v_i. The voltage across the inductor is given in (3). Capacitor and resistor does not get the current flow, where i_L is zero. This is similar to boost converter in ON state.

$$v_i = L\frac{di_L}{dt} \tag{3}$$

$$i_L = C\frac{dV_c}{dt} + \frac{V_c}{R} = 0 \tag{4}$$

Let $V_c= x_1$ and $i_L=x_2$. The state derivation of x'_1 and x'_2 in (5) and (6) can be gathered by rearranging (3) and (4). The state space matrix in (7) for buck boost converter in ON state can be formulated using (5) and (6).

$$x'_1 = \frac{1}{L}v_i \tag{5}$$

$$x'_2 = -\frac{x_2}{RC} \tag{6}$$

$$\begin{bmatrix} x'_1 \\ x'_2 \end{bmatrix} = \begin{bmatrix} 0 & 0 \\ 0 & -\frac{1}{RC} \end{bmatrix} \begin{bmatrix} x_1 \\ x_2 \end{bmatrix} + \begin{bmatrix} \frac{1}{L} \\ 0 \end{bmatrix} u_1 \tag{7}$$

During OFF state, it is similar to buck converter where v_1 is zero and its output state V_c and i_L are reverse in polarity due to inductor discharging as in (8) and (9) respectively.

$$-V_c = L\frac{di_L}{dt} \tag{8}$$

$$-i_L = C\frac{dV_c}{dt} + \frac{V_c}{R} \tag{9}$$

By expressing state variables $V_c= x_1$ and $i_L=x_2$. Its derivative x_1 and x_2 in (10) and (11) can be obtained by rearranging (8) and (9). The state space for buck boost converter in OFF state can be calculated using (10) and (11).

$$x'_1 = \frac{1}{L}x_1 \tag{10}$$

$$x'_2 = -\frac{1}{C}x_1 - \frac{1}{RC}x_2 \tag{11}$$

$$\begin{bmatrix} x'_1 \\ x'_2 \end{bmatrix} = \begin{bmatrix} 0 & \frac{1}{L} \\ -\frac{1}{C} & -\frac{1}{RC} \end{bmatrix} \begin{bmatrix} x_1 \\ x_2 \end{bmatrix} + \begin{bmatrix} 0 \\ 0 \end{bmatrix} u_1 \tag{12}$$

ISSN(Online): 2320-9801
ISSN (Print): 2320-9798

International Journal of Innovative Research in Computer and Communication Engineering

(An ISO 3297: 2007 Certified Organization)

Website: www.ijircce.com

Vol. 5, Issue 4, April 2017

The average of the buck boost converter for its ON and OFF state can be calculated with the account of duty cycle *d*. The average A and B matrix are shown in (13) and (14) respectively.

$$\bar{A} = A_{ON}d + A_{OFF}(1-d)$$

$$\bar{A} = \begin{bmatrix} 0 & 0 \\ 0 & -\frac{1}{RC} \end{bmatrix} d + \begin{bmatrix} 0 & \frac{1}{L} \\ -\frac{1}{C} & -\frac{1}{RC} \end{bmatrix} (1-d) = \begin{bmatrix} 0 & \frac{1-d}{L} \\ -\frac{1-d}{C} & -\frac{1}{RC} \end{bmatrix} \quad (13)$$

$$\bar{B} = B_{ON}d + B_{OFF}(1-d)$$

$$\bar{B} = \begin{bmatrix} \frac{1}{L} \\ 0 \end{bmatrix} d + \begin{bmatrix} 0 \\ 0 \end{bmatrix} (1-d) = \begin{bmatrix} \frac{d}{L} \\ 0 \end{bmatrix} \quad (14)$$

To finish the buck boost converter model, the substituted in equation (1). The final buck boost converter state space model is shown in (15).

$$\begin{bmatrix} x'_1 \\ x'_2 \end{bmatrix} = \begin{bmatrix} 0 & \frac{(1-d)}{L} \\ -\frac{(1-d)}{C} & -\frac{1}{RC} \end{bmatrix} \begin{bmatrix} x_1 \\ x_2 \end{bmatrix} + \begin{bmatrix} \frac{d}{L} \\ 0 \end{bmatrix} v_1 \quad (15)$$

The output state space for C and D matrix is shown in (16).

$$\begin{bmatrix} y_1 \\ y_2 \end{bmatrix} = \begin{bmatrix} 1 & 0 \\ 0 & 1 \end{bmatrix} \begin{bmatrix} i_L \\ V_C \end{bmatrix} + \begin{bmatrix} 0 \\ 0 \end{bmatrix} v_1 \quad (16)$$

III. BLDC MOTOR

The principle of the working of a brushless DC motor is the mechanical torque development due to the interaction of the magnetic field produced by rotor magnets and stator coils. The electronic switching or commutation circuit switches the supply to the stator windings such that one winding is energized with positive power, and the second winding with a negative power and the third is non-energized to develop the torque. So the peak torque occurs when these two fields are at 90 degrees to each other and get reduced when they move together (in terms of phase difference).

ISSN(Online): 2320-9801
ISSN (Print): 2320-9798

International Journal of Innovative Research in Computer and Communication Engineering

(An ISO 3297: 2007 Certified Organization)

Website: www.ijircce.com

Vol. 5, Issue 4, April 2017

The combined Clarke and Park Transformations can be written in Matrix form as:

$$\begin{bmatrix} I_d \\ I_q \end{bmatrix} = \frac{2}{3}\begin{bmatrix} \cos(\theta) & \cos(\theta - \frac{2\pi}{3}) & \cos(\theta + \frac{2\pi}{3}) \\ \sin(\theta) & \sin(\theta - \frac{2\pi}{3}) & \sin(\theta + \frac{2\pi}{3}) \end{bmatrix}\begin{bmatrix} I_a \\ I_b \\ I_c \end{bmatrix}$$

Where Id and Iq are the direct axis & quadrature axis respectively, θ is the angular position of the rotor. Likewise, the inverse transformation is given by:

$$\begin{bmatrix} I_a \\ I_b \\ I_c \end{bmatrix} = \begin{bmatrix} \cos(\theta) & -sin\theta \\ \cos(\theta - \frac{2\pi}{3}) & -sin(\theta - \frac{2\pi}{3}) \\ cos(\theta + \frac{2\pi}{3}) & -sin(\theta + \frac{2\pi}{3}) \end{bmatrix}\begin{bmatrix} I_d \\ I_q \end{bmatrix}$$

IV. MATHEMETICAL MODEL OF BLDC

The electrical and mechanical equations of the PMSM in the rotor (dq) reference frame are as follows:

$$V_d = R_s i_d + L_d \frac{di_d}{dt} - L_q I_q \omega_e \quad (1)$$

$$V_q = R_s i_q + L_q \frac{di_q}{dt} + \omega_e \lambda_{af+} L_d I_d \omega_e \quad (2)$$

By rearranging the terms in Equation (1) & (2), and then integrating them, we can obtain the equations for direct axis and quadrature axis currents.

$$i_d = \frac{1}{L_d}\int (V_d + L_q I_q \omega_e - R_s i_d) dt \quad (3)$$

$$i_q = \frac{1}{L_q}\int (V_q + L_q I_q \omega_e - R_s i_d - \omega_e \lambda_{af} - R_s i_q) dt \quad (4)$$

The mechanical equation can be written as:

$$T_e = \frac{3}{2} P\{\lambda_{af} I_q + (L_d - L_q)(I_d I_q) \quad (5)$$

$$\omega_e = \frac{P}{2J}\int \left(T_e - T_L - \frac{2B\omega_e}{P}\right) dt \quad (6)$$

Where Id is Direct Axis Stator Current in Ampere (A), Iq is Quadrature Axis Stator Current in Ampere (A),Rs is Stator Resistance in Ohms (Ω), Ld is Direct Axis Inductance in Henry (H), Lq is Direct Axis Inductance in Henry (H), J is Moment of Inertia in Kgm2, B is Friction Vicious Gain in Nm/rad/sec, P is Number of Poles, λaf is Rotor Flux Constant in V/rad/sec, ωe is Rotor's Electrical Speed in rad/sec, TL is Load Torque in Nm2, Te is Electromagnetic Torque in Nm.

ISSN(Online): 2320-9801
ISSN (Print): 2320-9798

International Journal of Innovative Research in Computer and Communication Engineering

(An ISO 3297: 2007 Certified Organization)

Website: www.ijircce.com

Vol. 5, Issue 4, April 2017

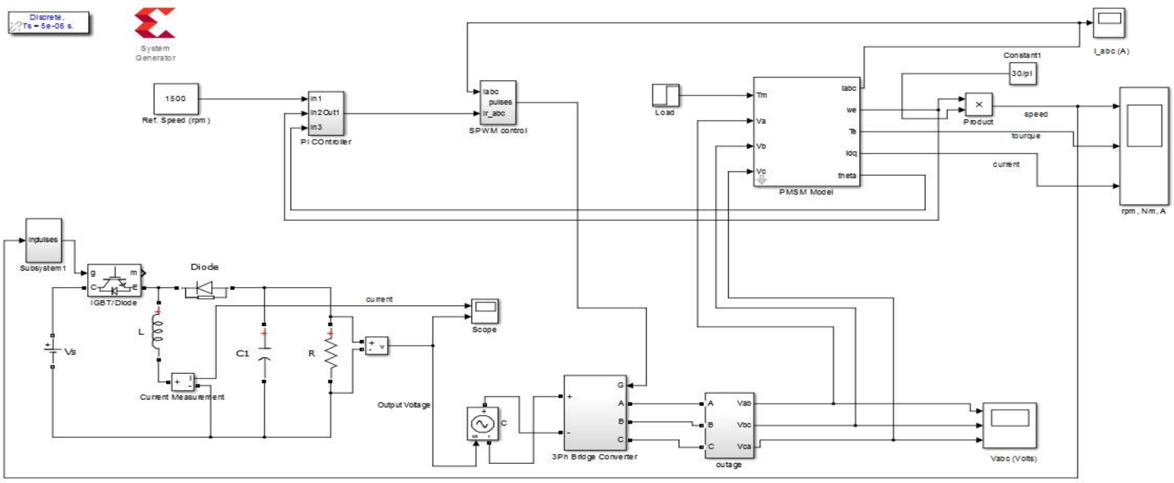

Figure2: Simulation model

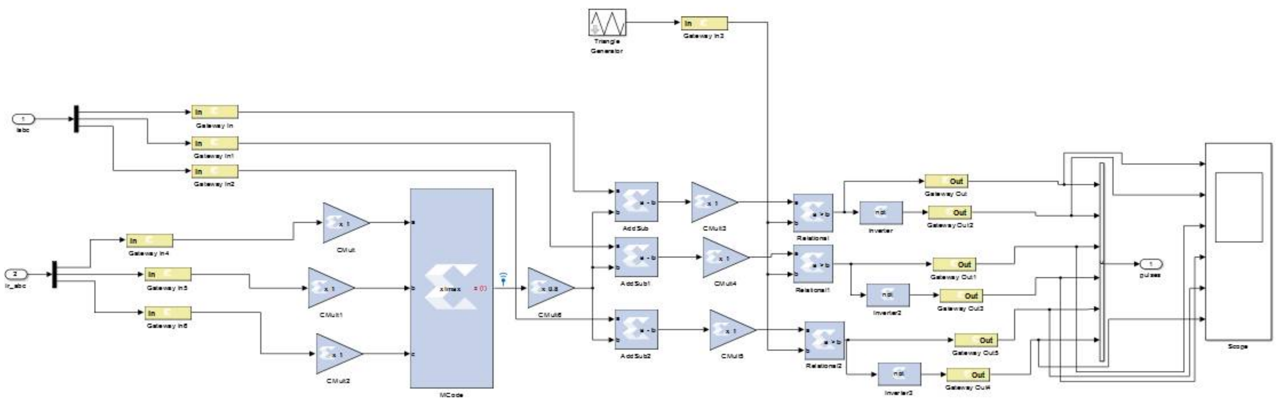

Figure3: Subsystem of SPWM Using Xilinx

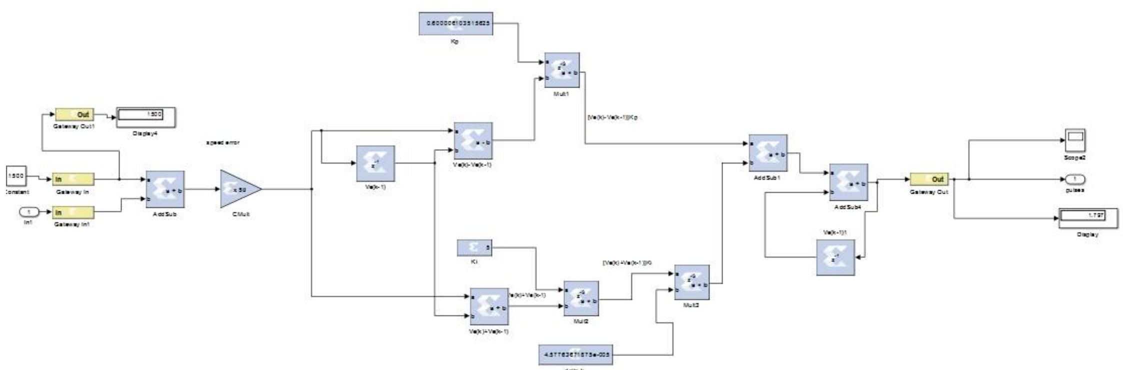

Figure4: PI controller for buck boost

ISSN(Online): 2320-9801
ISSN (Print): 2320-9798

International Journal of Innovative Research in Computer and Communication Engineering
(An ISO 3297: 2007 Certified Organization)
Website: www.ijircce.com
Vol. 5, Issue 4, April 2017

V. RESULTS

Simulation Runs have been carried out for various load cases. Here, we present two cases, one where the motor is started on load which remains constant throughout the operation, and another where the load applied is increased after some time has elapsed.

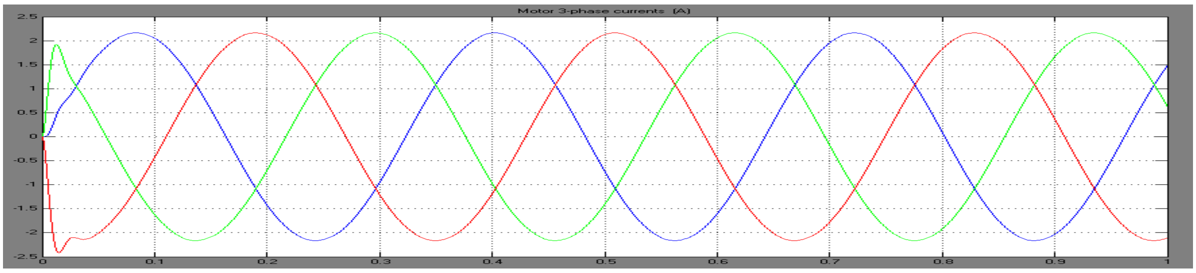

Figure 5: Phase Current Waveforms

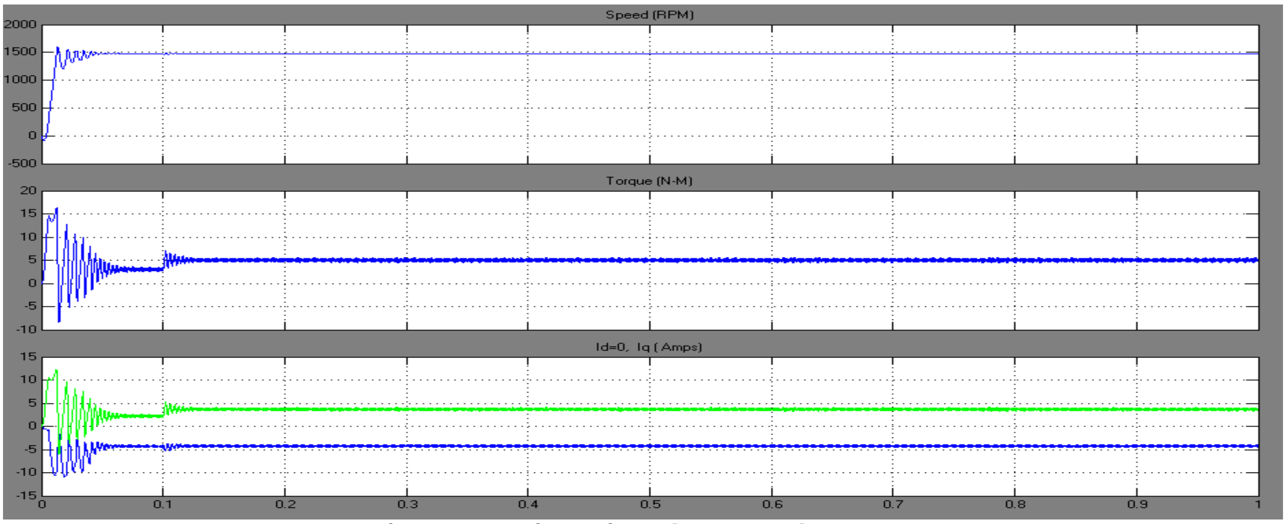

figure6: waveform of speed, torque and current.

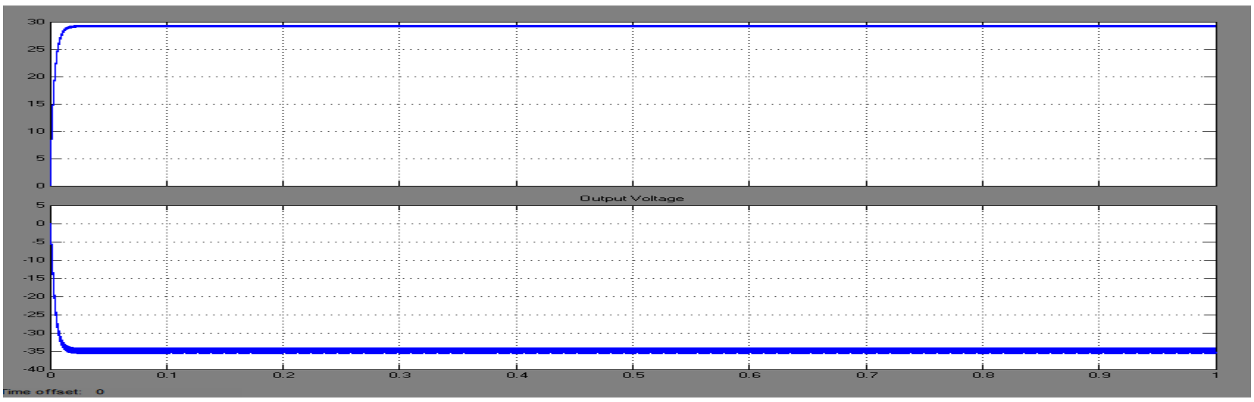

Figure7: buck boost converter output

ISSN(Online): 2320-9801
ISSN (Print): 2320-9798

International Journal of Innovative Research in Computer and Communication Engineering

(An ISO 3297: 2007 Certified Organization)

Website: www.ijircce.com

Vol. 5, Issue 4, April 2017

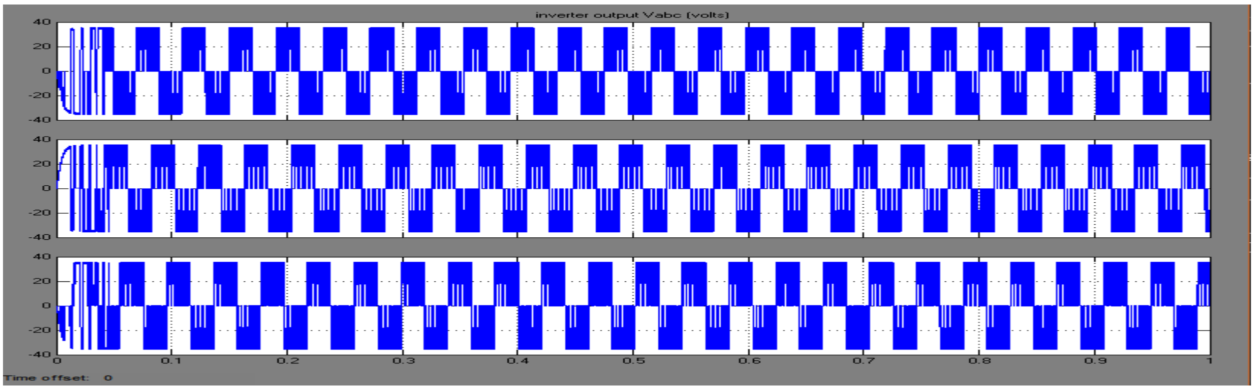

Figure8: inverter output voltage

VI. CONCLUSION

The dual loop control scheme, based on an FPGA, for speed control of a BLDC motor, targeting precise speed control and medium power application such as EVs and HEVs, has been presented in this paper. The proposed control scheme has the following advantages:1. Simulation results discussed so far illustrate the effectiveness of the control scheme in tracking the commanded speed in a very shorter time and with quite less speed ripple as well. 2. The main attractive feature of the proposed work is the easy and quick realization in real time applications when this control logic is implemented on the XSG platform. 3. The proposed FPGA based PI controller is sufficiently fast in its action of generating the desired dc link voltage from the buck{boost converter and hence the desired speed control. 4. Moreover, the average speed error and maximum speed error are evaluated in order to determine certain further applications of the proposed system. Therefore, the observed dynamic performance of the BLDC drive system has demonstrated the ability of the proposed control scheme to be selectively used for applications that require very high speed accuracy along with fast dynamic response such as biomedical/health care equipment, printing technology, and aerospace applications.
This paper, thus, illustrates the feasibility of an accurate speed controller along with the estimator portion of the controller. The implementation of a dual control loop to control speed either via changing dc link voltage with a PI controller or by changing the time interval for conduction state of phases facilitates end to end speed control. Hence the proposed model realized the speed controller for a BLDC motor, which is demanded increasingly, using the FPGA based control scheme. Finally the performance of the system is evaluated in MATLAB/SIMULINK software integrated with the Xilinx system generator.

REFERENCES

[1] Singh B, Singh S. State of art on permanent magnet brushless DC motor drives. J Power Electron 2009; 9: 1-17.
[2] Shah NP, Hirzel AD, Baekhyun C. Transmissionless selectively aligned surface-permanent-magnet BLDC motor in hybrid electric vehicles. IEEE T Ind Electron 2010; 57: 669-677.
[3] Luo FL, Yeo HG. Advanced PM brushless DC motor control and system for electric vehicles. In: IEEE 2000
Conference Record of the Industry Applications; 8{12 October 2000; Rome, Italy. New Jersey, NJ, USA: IEEE. pp. 1336-1343.
[4] Rajan AA, Raj RD, Vasantharathna S. Fuzzy based recon_gurable controller for BLDC motor. In: Computing In- ternational Conference on Computing, Communication and Networking Technologies; 29{31 July 2010; Tamilnadu, India. New Jersey, NJ, USA: IEEE. pp. 1-7.
[5] Singh B, Singh BP, Dwivedi SK. A state of art on different con_gurations of permanent magnet brushless machines. IEI J 2006; 78: 63-73.
[6] Rajagopal KR, Nair A. Design and development of a TMS320F2812 DSP controller based PM BLDC motor drive. In: International Conference on Electrical Machines and Systems; 10{13 October 2010; Songdo Convensia Incheon, South Korea. New Jersey, NJ, USA: IEEE. pp. 776-780.